SPIE 4669, 172-183 (2002) (Electronic Imaging 2002) 23 Jan 2002 LBNL-49316

Radiation events in astronomical CCD images *

A. R. Smith, R. J. McDonald, D. L. Hurley, S. E. Holland, and D. E. Groom
Lawrence Berkeley National Laboratory, Berkeley, CA 94720
W. E. Brown, D. K. Gilmore, R. J. Stover, and M. Wei
University of California Observatories/Lick Observatory,
University of California at Santa Cruz, Santa Cruz, CA 95064

ABSTRACT

The remarkable sensitivity of depleted silicon to ionizing radiation is a nuisance to astronomers. "Cosmic rays" degrade images because of struck pixels, leading to modified observing strategies and the development of algorithms to remove the unwanted artifacts. In the new-generation CCD's with thick sensitive regions, cosmic-ray muons make recognizable straight tracks and there is enhanced sensitivity to ambient gamma radiation via Compton-scattered electrons ("worms"). Beta emitters inside the dewar, for example high-potassium glasses such as BK7, also produce worm-like tracks. The cosmic-ray muon rate is irreducible and increases with altitude. The gamma rays are mostly by-products of the U and Th decay chains; these elements always appear as traces in concrete and other materials. The Compton recoil event rate can be reduced significantly by the choice of materials in the environment and dewar and by careful shielding. Telescope domes appear to have significantly lower rates than basement laboratories and Coudé spectrograph rooms. Radiation sources inside the dewar can be eliminated by judicious choice of materials. Cosmogenic activation during high-altitude flights does not appear to be a problem. Our conclusions are supported by tests at the Lawrence Berkeley National Laboratory low-level counting facilities in Berkeley and at Oroville, California (180 m underground).

Keywords: CCD, cosmic rays, high resistivity, fully depleted, astronomical, Lick Observatory, Lawrence Berkeley National Laboratory

1. INTRODUCTION

Most large detectors at high-energy physics colliders contain "vertex detectors" consisting of depleted silicon strip or pixel devices, sometimes with total areas of many square meters. The ability of ionizing radiation to generate electron-hole pairs in silicon is the bane of optical astronomy, where "cosmic rays" contribute confusion and loss of imaging pixels in CCD's. Multiple exposures and elaborate software are used to eliminate these artifacts.

Although astronomers tend to call all of these radiation events/objects "cosmic rays," genuine cosmic rays consist almost exclusively of muons produced by secondary meson decay. This is true even at the altitude of Mauna Kea, although at higher altitudes (e.g. jet aircraft cruising altitudes) the flux is dominated by protons and neutrons. The muons have mean energies of ∼2–3 GeV, and penetrate even meters of material without interaction or apparent slowing. But in addition there are other kinds of radiation artifacts. We believe that most of these are caused by Compton recoil electrons from the ambient gamma ray background. In some situations, such as when a high-potassium glass is present in the dewar, direct β rays (electrons or positrons) produced near the surface of the glass can strike the CCD. Evidence for these conclusions are presented below.

In the usual case, where stellar images are undersampled and hence show a prominent point-spread function (PSF) several pixels wide, the "objects" produced by radiation are distinctively sharp. In thinned CCD's (typically with a 20 μm-thick sensitive region) these objects/events tend to consist of counts in one or more pixels, in some cases in a straight line. Sometimes a small arc or kinked track can be seen.

* This work was supported by the U.S. Department of Energy under contract No. DE-AC03-76SF00098.
Author information for DEG: DEGroom@lbl.gov, http://www-ccd.lbl.gov

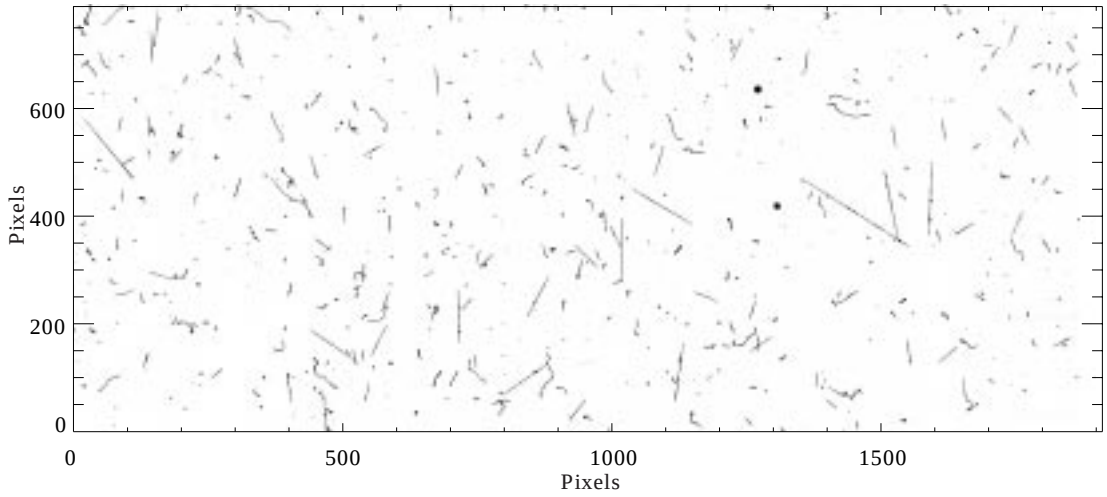

Figure 1. A 1980 pixel × 800 pixel subfield of a 3600 s dark exposure (totally depleted 270-μm thick LBNL CCD, NOAO CCD laboratory in Tucson), showing cosmic-ray muons (straight tracks), worms (low-energy electrons),and spots. While the spots look insignificant, they are about as abundant as the worms and can indicate considerable deposited energy.

With the advent of thicker high-resistivity CCD's,[1,2] the story is somewhat different. The cosmic-ray muon tracks are often quite long, and there is an abundance of wandering tracks which we call "worms." There are also localized events, usually but not always with fewer counts than would be expected from cosmic-ray muons, which we have called "spots." Muon tracks and worms are shown in Fig. 2.

The identification of the worms with multiple-scattered low-energy electrons is evident to people familiar with emulsion experiments. A 50-yr old example of a worm can be seen in Fig. 3.15.1 of Ref. 3.

We have made a study of these events, in most cases in totally depleted LBNL CCD's[1] 200-300 μm thick. Long (typically 1200 s) dark images were obtained at a variety of places, including deep underground, Kitt Peak, and Lick Observatory. In this paper we explore the nature of the events and the use of lead shielding to reduce the number of spots and worms. Appendices summarize the nature and intensity of cosmic rays and energy deposition by charged particles and gamma rays in CCD's.

2. EVENT CHARACTERIZATION

Figure 1 shows a 500 × 500 pixel subfield representing a 4000 s exposure in the Lick 3-m Coudé spectrometer room on Mt. Hamilton. The typical mix of muons (straight tracks), worms, and spots can be seen. We are interested in knowing not only the relative rates of different kinds of events, but the energy deposition and rate of pixel loss for each.

Software has been developed which is at least partly successful in making this characterization. Standard LBNL Supernova Cosmology Project programs have been used to isolate the events. Since a limited number of exposures have been obtained in each of several very different situations, it has not been practical to construct a superflat for background elimination. Instead, for each image a surfacing program was used to create a smooth background image via a boxcar averaging in which pixels with more than a few standard deviations above the mean were ignored. This image was subtracted from the input image, and the sky noise recalculated. Code used to identify and isolate stars and galaxies then isolated and tabulated the radiation events. An isolated event is defined as a group of connected pixels with counts more than some number of standard deviations above background (typically at 1.5 or 2 σ), with at least one pixel having a significantly higher number of counts, typically 5 σ above background. This code generated a number of parameters for each object, including the second moments of the distribution about the centroid.

Energy deposition by charged particles is discussed in Appendix B. Most of the cosmic-ray muons are just above "minimum ionizing;" that is, they have energies such that the ionization rate dE/dx is slightly above the broad minimum shown in Fig. 13. (The most probable energy loss is even more independent of energy in this

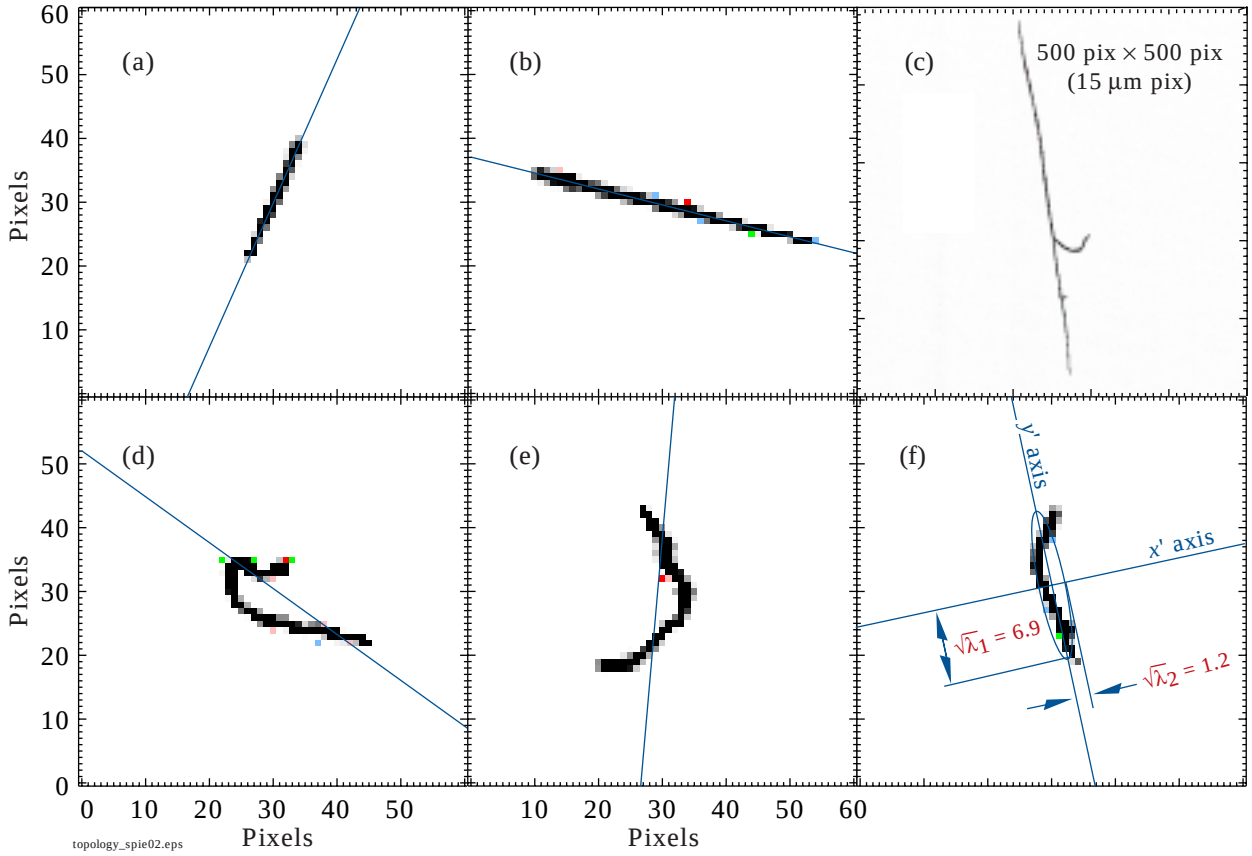

Figure 2. Examples of cosmic-ray muons (a–c) and worms (d–f) in a totally depleted 200-μ thick LBNL CCD. (c) shows one of the longest tracks found, and two δ rays (knock-on electrons) can be seen. (f) also indicates the the definition of λ_1 and λ_2, the principal moments of the distribution.

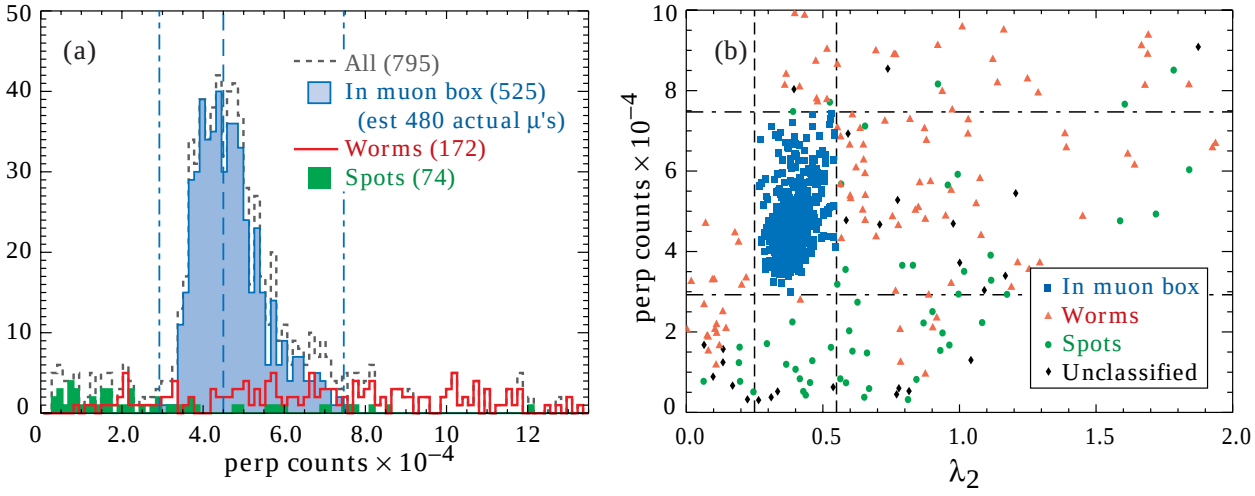

Figure 3. Total exposure of 4800 s at the LBNL Low Background Facility (LBNL LBF). (a) Distribution of the normal projection of the number of counts ("perp counts"). The estimated position of the minimum-ionization most probable loss is indicated by the dashed line, and the cuts chosen for the "muon region" are shown by the dash-dotted lines. (b) Distribution of "perp counts" as a function of the smallest eigenvalue λ_2. The minimum-ionization cut and the additional cut $0.25 < \lambda_2 < 0.55$ define the "muon box."

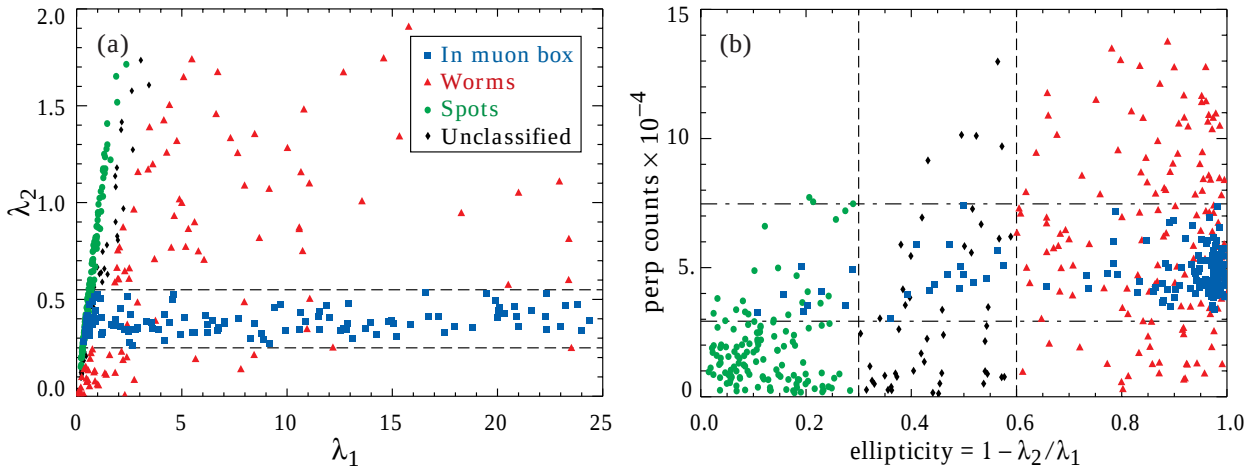

Figure 4. (a) λ_2 vs λ_1 and (b) "perp counts" vs ellipticity for a long dark exposure in the UCO/Lick CCD laboratory, where the Compton rate was more than twice the cosmic-ray muon rate.

region.) If the number of counts in a cosmic-ray event is scaled by the wafer thickness divided by the track length, as calculated from the observed projected length, this number should be the same for all cosmic rays. For lack of a good name, we call it "perpendicular counts" or "perp counts."

The distribution of this quantity for a series of long dark exposures at the LBNL Low-level Background Facility (LBF)[4] is shown in Figure 3(a). The distribution is broadened by both fluctuations in the energy loss (the "Landau tail" on the high-energy side) and energy escape. The vertical dashed line in Figure 3 indicates the most probable number of counts. The vertical cuts above and below the peak are chosen conservatively to include essentially all of the muons.

A muon track should be a straight line. A measure of "straightness" can be obtained from the second moments matrix. One can imagine rotating the coordinate system, as shown in Figure 2(f), so that the matrix is diagonal. With the labels as shown, the $y'y'$ moment is minimal for a straight line (muon), while the $x'x'$ moment can have any value. The $x'y'$ moment is zero, by the definition of the transformation. These moments are simply the eigenvalues of the original matrix, and the transformation does not need to be made explicitly. We define λ_1 (λ_2) as the minimal (maximal) eigenvalue of the second moments matrix, normalized by dividing by total number of counts in the event so that the result is independent of amplifier gain.

A plot of "perp counts" as a function of λ_2 for the muon-rich exposures at the LBF is shown in Fig. 3(b). In this case most cosmic-ray muons are in the interval $0.25 < \lambda_2 < 0.55$; in other situations limits of this band vary because of different CCD bias, thickness, and other factors. Our "muon box" is defined by the cuts on "perp counts" and λ_2. Non-muon events similar to those outside the box also occur inside, although in this example the estimated contamination is less than 10%. Hand-scans of a muon-free run (discussed below) verify that non-muon events in this box are genuinely indistinguishable from muons. On the other hand, some muons escape from the box. Scanning shows these to be mostly unusual muon events with a small δ-ray track or other artifact superimposed on the evident muon track.

The distribution of λ_2 vs λ_1 (Fig. 4(a)) is diagnostic, although it is not used in selection cuts. The muon band is evident. Since $\lambda_1 \geq \lambda_2$, spots cluster along the diagonal. A lower cut on λ_1 would eliminate some contamination in the muon box but would cause unacceptable muon loss.

The secondary quantity e (ellipticity) $= 1 - \lambda_2/\lambda_1$ is also useful; the distribution "perp counts" vs e is shown in Fig. 4(b). As expected, most muons cluster at large e, although a cut on this quantity is not useful because near-normal muons have small eccentricity and would be lost. The somewhat arbitrary definitions of spots as events with $e < 0.3$ and not in the muon box, and worms as events with $e > 0.6$ and not in the muon box, are useful, since the abundance of each is very site-dependent and therefore interesting.

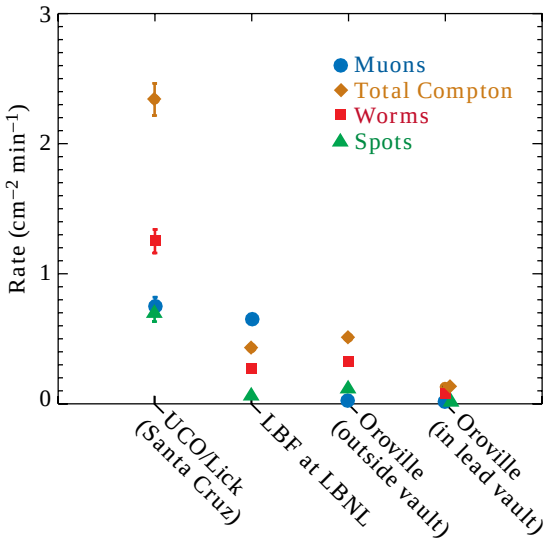

Figure 5. Summary of experiments to establish that the "worms and spots" were not related to cosmic rays but were related to environmental γ-ray sources.

3. THE NATURE OF COSMIC RAYS, WORMS, AND SPOTS

Four sets of long dark exposures were obtained, using the same CCD and dewar:

1. In the basement of the UCO/Lick CCD laboratory in Santa Cruz. Almost half the events were muons (at the expected rate); the remainder was worms and spots.

2. In the LBNL Low Background Facility (a room with 1.5 m thick concrete walls; the special concrete has very low radioisotope content) Almost entirely muons; results of these exposures were shown in Fig. 3.

3. Near the power plant of the Oroville (California) dam, 480 meters-water-equivalent (mwe) underground, where cosmic rays are attenuated by 10^3. Worms and spots were observed, but no muons.

4. Again at Oroville, but this time in a lead vault built for demanding low-level counting experiments. This time almost nothing was observed—171 events in 8400 s. Since the site is ultraclean, these few counts are assumed to originate in the dewar assembly.

These results, summarized in Fig. 5, together with the track topology, are consistent with the non-muon components being Compton-scattered electrons from ambient gamma rays—from the decay of inevitable trace amounts of uranium, thorium, and the radioisotopes in their decay chains. ^{40}K is also present, and may even be the dominant contributor. 11% of the time it decays to ^{40}Ar with the production of a 1.46 MeV photon, and 89% of the time to ^{40}Ca by β^- emission (1.33 MeV endpoint).

Gamma rays are very penetrating (see Fig. 12), while β-decay electrons are stopped by small amounts of material. Even at the endpoint energy, the β^- has a range of only 620 μm.[5] Alpha particles (^{4}He ions) are energetic (5$\sim$10 MeV), have small range ($\sim$ 30 μm), but are of concern if the semiconductor substrate contains an α-emitting nuclide.

4. BACKGROUND AT THE LICK 3-M SPECTROMETER: SHIELDING

A 200-μm-thick LBNL depleted CCD is in use at the Lick 3-m Coudé spectrometer. Early test data indicated expected muon rates but Compton rates several times greater, 1.6 cm^{-2} min^{-1}. In subsequent experiments long dark exposures were obtained with 1/16 lead sheet wrapped around the dewar to obtain the desired absorber thickness. The results are shown in Fig. 6. As shielding was added the muon rate remained constant at

$0.8\ \mathrm{cm}^{-2}\,\mathrm{min}^{-1}$, indicating that the selection procedure was moderately robust against changes in the Compton rate. Spots were attenuated more easily than worms, and the total Compton rate reached about 0.7 of the cosmic-ray muon rate when 3/8 in (≈ 1 cm) of lead was used. (The rate increase at the last shielding thickness shown in the figure is not understood.)

A cryogenic germanium gamma spectrometer was taken to Mt. Hamilton, and spectra were obtained at approximately the dewar position in the spectrometer room. Spectra with no shielding and with 1 cm lead shielding are shown in Fig. 7. The naked spectrometer spectrum is as expected, with multiple lines at the gamma energy for complete energy containment, and a less-energetic continuum for partial containment events—those in which one or more Compton interactions occurred in the germanium, with the scattered gamma ray finally escaping. Except for the dominant ^{40}K line at 1460 keV, all the lines can be identified as nuclear gamma rays from the decay of uranium and thorium daughters. The continuum at low energies is higher than would be expected by these mechanisms, which is understood to be the result of degradation of photon energies via Compton scattering in the walls and floor of the room.

The shielding was very effective in attenuating low-energy gamma rays and had little effect above about 1.5 MeV, as might be expected from Fig. 12. However, the higher-energy gamma rays have little interaction probability near or in the CCD. The lower-energy (0–1000 keV) photons, which were most attenuated, were those to which the CCD is more sensitive. The four orders of magnitude of the vertical logarithmic scale are deceptive: The counting rate was decreased by 80% by the 1 cm lead shield. The appearance of the fluorescence lead K x-ray peak at 88 keV is reassuring and does not pose a problem, since these photons are absorbed by the dewar wall.

A reasonable criterion for adequate shielding might be that the Compton rate is lower than the irreducible cosmic-ray muon rate. This is relatively easy to achieve without too much added weight.

The apparent peak in the unshielded spectrum at ≈ 100 keV is not understood; that it is not a threshold effect is shown by spectra obtained elsewhere with this spectrometer, and the fact that the attenuated spectrum obtained under otherwise identical conditions does not show it. The "perp counts" and ellipticity plots for the first two (least shielding) of the dark exposure series are shown in Fig. 8.

The most probable energy loss for a muon traversing 200 μm of silicon should be about 78 keV, so the unusual low-energy peak in Fig. 8 is consistent with a $10 \sim 15$ keV energy deposition. These events appear as the spots at the lower left corner of the ellipticity plot, Fig. 8(b).

5. KITT PEAK 4-M RC/MARS SPECTROMETER ENVIRONMENT

Arjun Dey and collaborators are using an 800×1980 LBNL CCD in the Mayall 4-m RC/MARS spectrometer at Kitt Peak, and have supplied long dark CCD exposures in various orientations at the telescope and in the NOAO laboratory in Tucson. The Compton rates at the telescope are nearly identical with the muon rates, so the shielding provided by the steel floor and absence of overhead sources seems to shield the camera effectively. In at least this case the Compton rate is acceptable. Exposures in the Tucson NOAO lab yielded the highest radiation rates we have seen except when a radioactive source is present.

Rates increased dramatically when a field lens was added inside the dewar. With the same lens just outside the dewar, the excess rate disappeared. We have since assayed this lens and found that the BK7 glass contains 11% potassium. The CCD was exposed to direct beta rays (e^-) produced near the surface of the glass from $^{40}\mathrm{K} \rightarrow {}^{40}\mathrm{Ca}$ decays.

6. LINCOLN LABS/MIT CCD'S

Long dark exposures were made at UCO/Lick with LL/MIT CCD20, a deep-depletion device intended for the DEIMOS spectrometer at the Keck Observatory.[2] The sensitive thickness is estimated as 40 μm. Distributions of "perp counts" and "perp counts" vs λ_2 are shown in Fig. 9. The cosmic-ray minimum ionization peak is clearly visible, albeit much broader than we obtain with the 300 μm LBNL CCD's. Much of the increase is caused by our algorithm's difficulty in obtaining a meaningful normal projection of the number of counts.

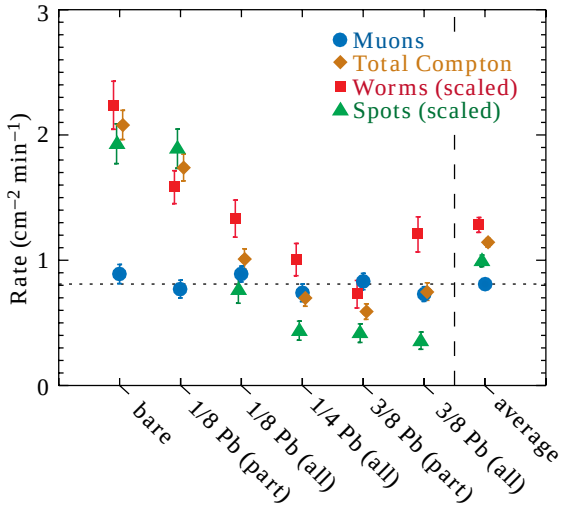

Figure 6. Rates of cosmic-ray muons and Compton electrons, and relative rates of worms and spots, in the Lick Observatory 3-m Coudé spectrometer room, as a function of increasing amounts of lead shielding around the dewar. This particular CCD was 200 μm thick. Note that the worm and spot rates have been scaled to expedite comparison with the total Compton flux.

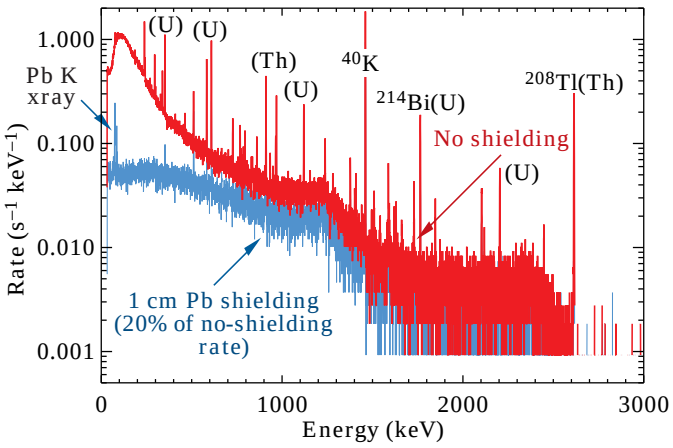

Figure 7. Gamma spectra in the Lick 3-m Coudé spectrometer room, without and with a 1-cm lead shield. Characteristic lines corresponding to emissions in ^{40}K decay and the U, Th decay chains can be seen, plus a continuum due to partial-containment events and to photons degraded by previous scattering.

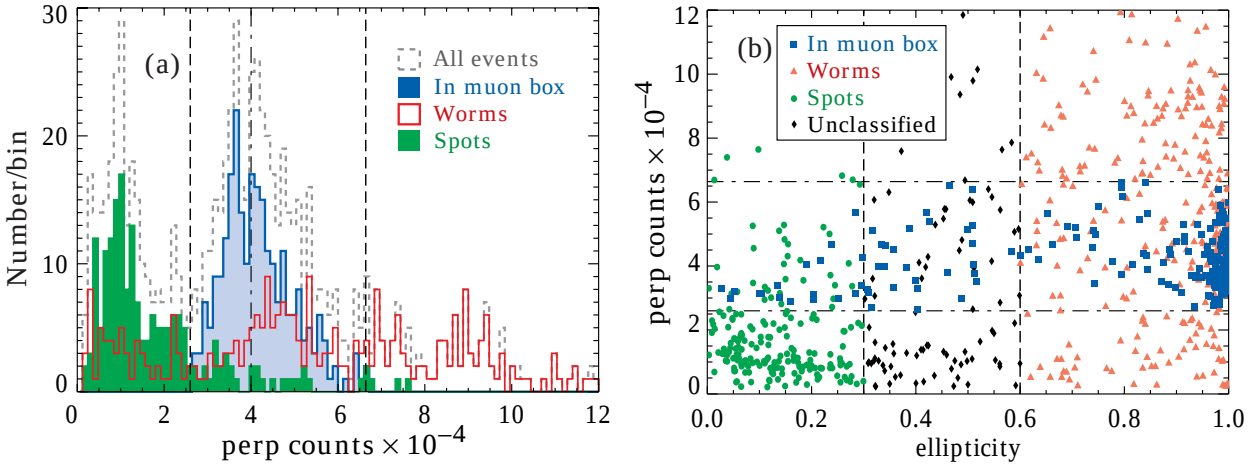

Figure 8. (a) "Perp counts" spectrum and (b) "perp counts" vs ellipticity for the two Mt. Hamilton 3-m spectrometer dark exposure series with least shielding.

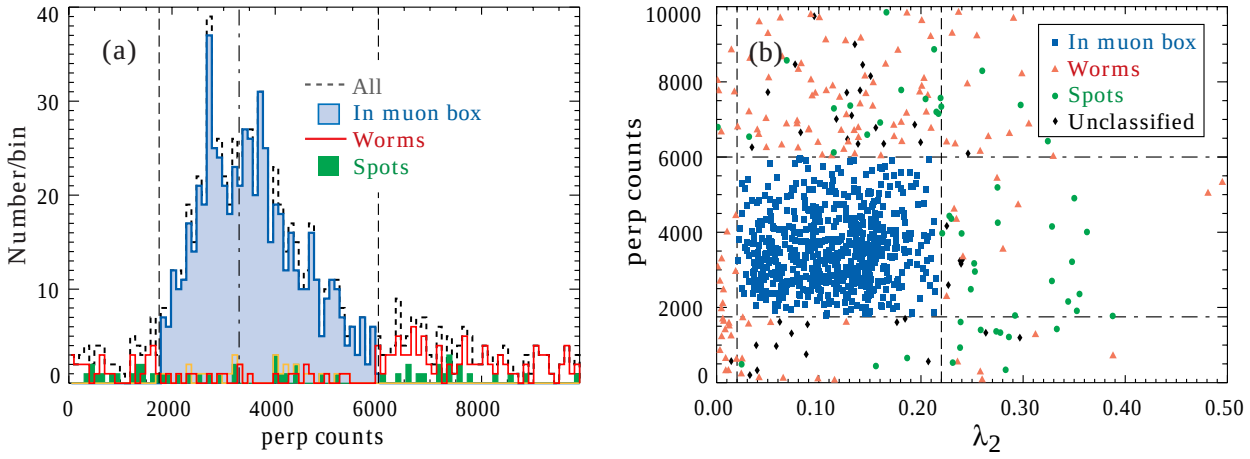

Figure 9. (a) "Perp counts" spectrum and (b) "perp counts" vs λ_2 from two long dark exposures of LL/MIT CCD20, a deep depletion device. The exposures were obtained at UCO/Lick in a reasonably dirty environment.

The muon box is so large that a clean muon/Compton separation is not possible, but with both the LBNL CCD (270 μm thick) and a lead-shielded (5 cm) LL/MIT CCD, we obtain a muon flux of (0.93 ± 0.07) cm^{-2} min^{-1}(with systematic errors which are not very well known). Assuming this background, the ratio of Compton rates for an unshielded LL/MIT thick CCD to that in the LBNL CCD is 0.65, with $\sim$ 10%–15% uncertainty. The thickness ratio is 0.15. The difference provides evidence that many of the Compton recoil electrons do not originate in the sensitive volume of the CCD. Sensitivity to Compton recoil electrons (and direct β rays if potassium is present in the dewar) is not limited to thick CCD's.

Table 1. Radiological assay results for common materials found in CCD dewars and nearby concrete. Numbers in parentheses indicate the error in the last place.

Sample	U (ppm)	Th (ppm)	K (%)
CCD black socket	0.64(4)	1.38(6)	0.011(1)
Si wafers (3 in box)	0.025(6)	0.16(2)	ND
Aluminum nitride	0.010(2)	0.019(5)	ND
Aluminum sputter	ND	0.044(14)	ND
Circuit boards (Lick)	0.064(4)	2.07(8)	0.016(2)
Epoxy (Lick)	0.012(3)	0.010(3)	ND
INVAR, bar stock	ND	ND	ND
Molybdenum, bar stock	0.020(3)	0.020(3)	ND
Sn/In alloy	5.0(1)	4.6(1)	ND
Lick 3-m core	1.35	4.0	0.72
UCO/Lick lab core	1.2	1.2	1.23
Mauna Kea lava	1.5	4.7	1.52

7. ASSAY RESULTS

We have characterized the U, Th, and K content of most materials in the dewar which might act as radiation sources. The results are given in the upper section of Table 1. The "black socket" for our test CCD was a radiation source, as seems to be common for materials with black dye. We use a thin ($\sim$500 Å) In/Sn coating as a rear window in our CCD's. Indium is naturally radioactive. While the Sn/In alloy is significantly radioactive, the amount used for the CCD windows is too small to cause a detectable effect.

We also characterized the concrete at the Lick 3-m telescope and the lava used as concrete aggregate at the Keck and other telescopes on Mauna Kea; these results are given in the lower part of Table 1. In both the Lick 3-m and UCO/Lick environments the Compton rate was 2.2 $cm^{-2}\,min^{-1}$, in contrast to 0.8–0.9 $cm^{-2}\,min^{-1}$ for cosmic rays. In rooms or dome floors made from such concrete, gamma attenuation by a factor of three or more would be desirable.

Conversion of the radionuclide content to activity is easily done for potassium, but is complicated by the decay chains for uranium and thorium. The conversions factors are 0.33 (pC/g)/ppm for uranium, 0.11 (pC/g)/ppm, and 8.5 (pC/g)/percent for potassium.

8. COSMOGENIC ACTIVATION

The same CCD/dewar that was used in the LBNL LBF experiments was taken to the Keck telescope on Mauna Kea to evaluate the radiation situation there. The results are confusing and as yet unexplained. Muon rates are consistent with the expected flux of 2 $cm^{-2}\,min^{-1}$. However, there was a significant worm component which was curiously insensitive to whether the dewar was in a lead box or not. One admittedly remote possibility was that the dewar itself was slightly radioactive, perhaps having been activated by cosmic rays at the jet cruising altitude (∼10–11 km) during the flight from San Francisco to Hawaii. At this altitude the much higher cosmic-ray flux is predominantly neutrons and protons, which could easily induce activity.[6] Such effects have been obseved and studied at near sea level,[7] and codes are available to simulate the activation.[8]

We found little guidance about cosmogenic activation at high altitudes, except the warning that experimenters who need ultra-low activity go to great lengths to avoid apparatus being transported by air. Accordingly, a simple experiment was done to study the possibility: Samples of the same stainless steel alloy used in the dewar were obtained in the form of 1.3 cm thick plates cut to fit around the LBNL LBF germanium gamma-ray spectrometer (a total of 7.3 kg). After characterization at the LBNL LBF underground facility[4] in Oroville, California, it was shipped by overnight delivery on two round trips from San Francisco to Boston during a 5 day interval. It was then immediately assayed at Oroville. The results were completely negative, but should provide reassurance to astronomers who ship radiation-sensitive apparatus by air. Although ^{44m}Sc, ^{51}Cr, ^{52}Mn, ^{54}Mn, ^{56}Co, ^{58}Co, and ^{60}Co not present before the flight were identified, rates were several orders of magnitude below rates measured in rock in concrete.

9. OBSERVATIONS AND CONCLUSIONS

We are not the first to find non-cosmic-ray events in CCD's, nor the first to recognize the distinctive energy deposit of a (normally incident) cosmic-ray muon.

In his 1986 review,[9] Mackay discusses the excess of rate over that expected from cosmic rays, and diagnoses much of the problem in one case as radiation from the glass window on the dewar. He reports rates of 10 $cm^{-2}\,min^{-1}$, more than 10 times the cosmic-ray rate.

An old ESO report lists cosmic-ray rates in a dozen CCD's ranging from 6 $cm^{-2}\,min^{-1}$ in RCA SIC 501 CCD's to 1.4 $cm^{-2}\,min^{-1}$ in a GEC 8603.[10]

Florentin-Nielsen and Anderson[11] describe experiments in which the device was operated 37 m below ground level in a chalk mine, with a reduction to 33% of the surface rate, to 0.56 $cm^{-2}\,min^{-1}$. The depth in mass/area^2 and the CCD orientation are uncertain, so we cannot comment on the residual non-cosmic-ray rate. In other experiments they identified a UBK-7 lens as producing very large rates because of its ^{40}K content.

Deep-depletion CCD's have been used in x-ray astronomy for a long time. Walton et al. describe a study[12] in which the minimum ionizing signal is used to discriminate against cosmic rays—the x-ray mirror response cut off at 10 keV, and only 10% of the cosmic-ray signals were this small.

There is anecdotal evidence of hotspots in a concrete telescope pier (Hugo Schwartz, reported on CCD-world) and drywall (Roy Tucker, reported on CCD-world), radioactive dewar windows (BK7 seems notorious in this regard because of its high potassium content), thorium-containing lenses, and the continued worry about radioisotope tracers used in process control. For example, in steel production ^{60}Co pellets are placed near the

outside of the furnace wall. When the firebrick gets thin enough, the radiation signature disappears and signals that the lining should be replaced.

Our study is unique, however, in that we are using much thicker CCD's than have previously been available, so that the events leave identifiable signatures. It is possible to do a moderately good job in isolating the muon and non-muon components. A series of experiments enabled us establish the Compton-scattered nature of the unwanted component—except for the interesting case of direct beta detection when ^{40}K-containing glass was "visible" to the CCD.

The study again emphasizes the need for care and careful characterization for every material used in the vicinity of the CCD, especially inside the dewar. The ubiquitous U and Th decay chain gammas are everywhere, but can be reduced below the cosmic-ray rate by careful shielding.

But we are left with mysteries: Shielding usually worked as expected, but in some cases had no apparent effect. Further work continues.

APPENDIX A. COSMIC RAYS

The vertical flux of cosmic rays in the atmosphere as a function of composition and height is shown in Fig. 20.3 in Ref. 6. At sea level 98% of cosmic rays are muons with a mean energy of about 4 GeV, while most of the rest are protons and neutrons. The muons are decay products of mesons produced in hadronic cascades initiated by primary cosmic rays, usually protons. Maximum intensity occurs at an altitude of about 10 km, and for $E \geq 1$ GeV there is an approximately exponential decrease below 500 g/cm^2 (≈ 6 km), with the vertical intensity at atmospheric depth h given by $I(h, \theta = 0) \approx 420 \times 10^{-h/(1330\,\mathrm{g/cm^2})} \mathrm{m^{-2}\,s^{-1}sr^{-1}}$. The vertical intensity at sea level for $E \geq 1$ GeV is 0.0072 cm^{-2} s^{-1}sr^{-1}. The vertical intensity at the top of Mauna Kea (4.3 km = 600 g/cm^2) is about 2.0 times higher.[†]

The differential spectrum[13, 14] at low momenta[‡] is shown in Fig. 10, and the integral vertical intensity (I_0) as a function of absorber thickness in in Fig. 11. Conversion of momentum thresholds to depth was made with the aid of the range-energy tables given in Ref. 16. In most situations there is some overburden (concrete floors above the laboratory or the apparatus itself), which must be estimated. The difficulty in estimating near-surface flux is compounded by the differences between published measurements below 1 GeV/c and by geomagnetic effects.

At low energies the angular distribution is usually approximated as $\cos^\alpha \theta$, where θ is the zenith angle, and $\alpha \approx 2$ for $E \sim 3$ GeV. The exponent decreases with energy and approaches -1 for energies $\gg 100$ GeV (see the review by Gaisser and Stanev, Sec. 20 of Ref. 6). The expected rate per unit area in a horizontal CCD is given by $R_{\mathrm{horiz}} = 2\pi\, I_0 \int_0^1 \cos^\alpha \theta \cos\theta\, d(\cos\theta) = 2\pi\, I_0/(\alpha{+}2)$. In the case of a vertical CCD, $R_{\mathrm{vert}} = 2I_0\, B(3/2, (\alpha{+}2)/2)$, where $B(\nu, \mu)$ is a beta function. For $\alpha = 2$ this function is $\pi/8$, so the rate is exactly half of R_{horiz}. Our measurements are in agreement with this observation.

In the situations of interest, the overburden is such that the threshold energy is considerably less than 1 GeV. From Fig. 11 we see that a vertical integral intensity of 0.009–0.010 cm^{-2} s^{-1}sr^{-1} would be more appropriate. The corresponding rate in a horizontal CCD should thus be 0.84–0.94 cm^{-2} min^{-1}. We in fact observe $(0.93 \pm 0.02_5)$ cm^{-2} min^{-1} at Santa Cruz, with some possible contamination in the muon box, and 0.71 ± 0.03 cm^{-2} min^{-1} at the LBNL LBF. In the latter case the vertical overburden is 3.8 mwe and the slant overburden greater; the observed flux is a little high but not by much. At Lick, at $h = 1290$ m ≈ 846 g/cm^2,* the intensity should be 33% greater than at sea level, and the CCD in the spectrometer is inclined at 53°. We regard the observed rate, (0.81 ± 0.03) cm^{-2} min^{-1}, as within expectations.

[†]The "U.S. Standard Atmosphere" is plotted in Ref. 3 (Fig. A.6.1) and tabulated in Ref. 15 (Table 3d-2).

[‡]Momentum (p) and energy (E) are related by $p^2c^2 = m_\mu^2 c^4 + E^2$, and the kinetic energy T is $E - m_\mu c^2$. Since $m_\mu c^2$ = 0.105658 GeV, T and pc differ by only 10% at $E = 1$ Gev, and they converge rapidly with increasing momentum. For our present purposes the difference can be neglected.

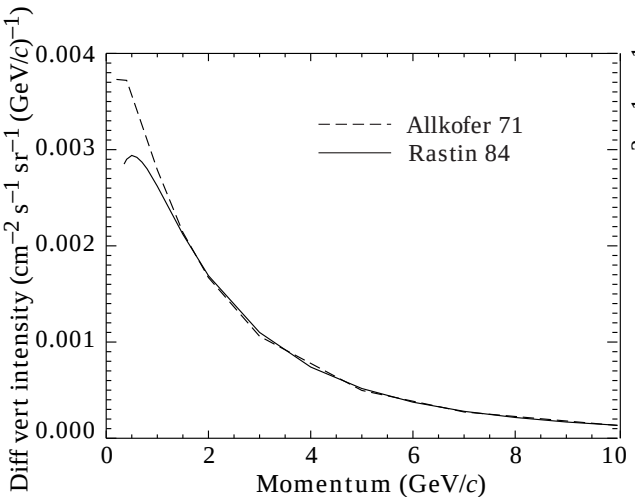

Figure 10. Differential cosmic-ray muon spectrum at sea level.

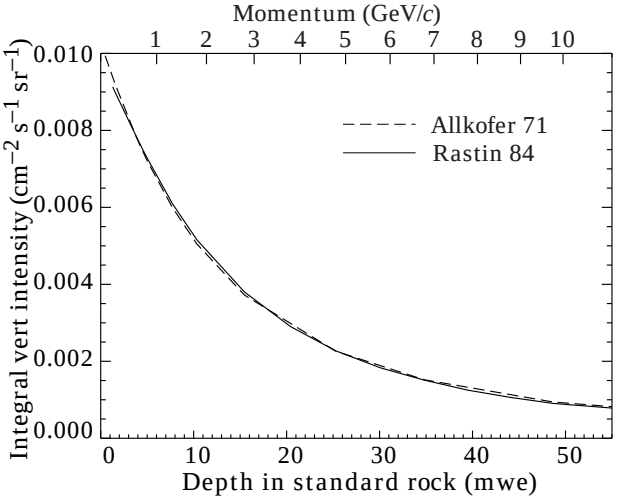

Figure 11. Integral spectrum of vertical muons as a function of depth in standard rock (ρ = 2.65 g/cm^3), expressed in meters-water-equivalent (mwe). The minimum momenta required to reach the given depths are shown by the top scale.

APPENDIX B. ENERGY LOSS OF ELECTRONS AND MUONS IN CCD'S

Figure 12 shows contributions to the photon mass attenuation coefficient in silicon.[5] The energies of photons in the places of interest are in 100–1000 keV region indicated by the shading. (The photon from ^{40}K $\rightarrow$ ^{40}Ar is at 1461 keV.) Compton scattering is seen to be the dominant process. A measure of the "transparency" of the materials can be obtained: The interaction probability of a 100 keV in 300 μm of silicon is 1.28%, and at 1 MeV it is 0.044%. The dewar is more transparent to higher-energy photons, but these scatter in the CCD with less probability. Most of the interactions involve very low-energy photons.

The mean rate of energy loss for muons and electrons in silicon is shown in Fig. 13. $\langle dE/dx \rangle$ at minimum ionization for muons (and for protons) is 1.664 MeV g^{-1}cm^{-2} = 387 eV/μm. We take the mean energy required to produce one e-h pair as 3.73 eV,[17] so that a mean of 31,200 e-h pairs are produced by the passage of minimum-ionizing muon through 300 μm of silicon. The energy loss is subject to fluctuations, leading to a fairly wide "Landau" distribution which is skewed to high energy loss. The details are thickness-dependent, but in 300 μm the most probable energy loss is 0.66 of this value,[18] or 20,600 e-h pairs. The most probable energy loss is quite insensitive to energy, much moreso than $\langle dE/dx \rangle$ itself.

We have independently calibrated the energy scale to much greater accuracy by observing the 56.378 keV gamma ray from a ^{241}Am source (actually from the ^{241}Np decay to its ground state). The results are in good agreement.

REFERENCES

1. S. E. Holland et al., "A 200 x 200 CCD Image Sensor Fabricated on High-Resistivity Silicon," IEDM Tech. Digest, 911 (1996); S. E. Holland et al., "Large Format CCD Image Sensors Fabricated on High Resistivity Silicon," *Proc. 1999 IEEE Workshop on Charge-Coupled Devices and Advanced Image Sensors*, 179-182, June 10-12, Karuizawa, Nagano, Japan (1999).
2. B. E. Burke et al., "Large-area back-illuminated CCD imager development," *Optical Detectors for Astronomy*, Kluwer Academic Publishers, Dordrecht, 19-28 (1998); B. E. Burke et al, "CCD imager technology development at Lincoln Laboratory," *Optical Detectors for Astronomy II*, Kluver Academic Publishers, 187-199 (2000).

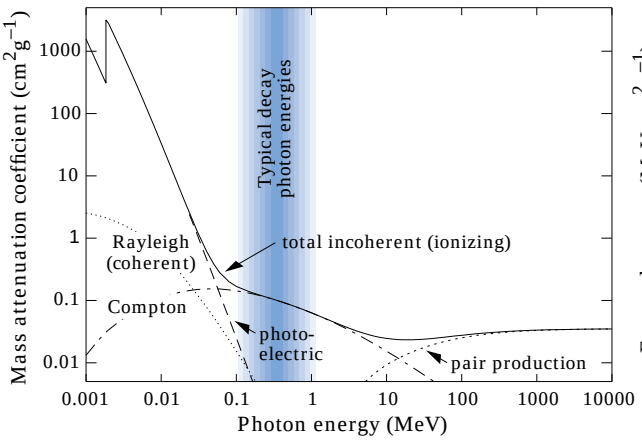

Figure 12. Mass attenuation coefficient of x rays/γ-rays in silicon.[5] An attenuation length of 1 cm^{2}g^{-1} corresponds to an interaction probability of 7% for a path length of 300 μm. The region of interest for this work is shaded.

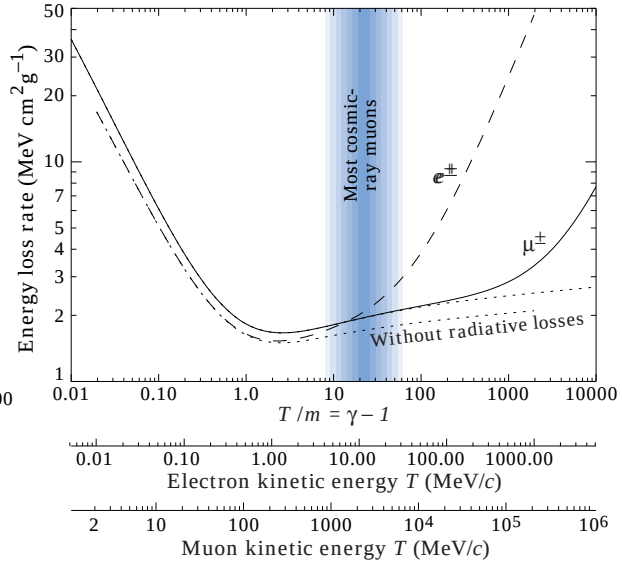

Figure 13. Mean energy loss rate of electrons and cosmic-ray muons in silicon. Most energy lost radiatively is not deposited in the silicon, so the curves without radiative losses should be used.

3. B. Rossi, *High Energy Particles*, (Prentice-Hall, Inc., Englewood Cliffs, NJ 1952).
4. `http://user88.lbl.gov/lbf/index.htm`
5. `http://physics.nist.gov/PhysRefData/`
6. D.E. Groom et al., *The Review of Particle Physics*, Euro. Phys. J. C15, 1–878 (2000) and 2001 off-year partial update for the 2002 edition available on the PDG WWW pages at `http://pdg.lbl.gov/`.
7. D. Lal & B. Peters, *Handbuch der Physik* 46/2, 551-612 (1967).
8. C. J. Martoff & P. D. Lewin, Comput. Phys. Commun. **72**, 96-103 (1992).
9. C. D. Mackay, *Ann. Rev. Astron. Astrophys.* **24**, 255–283 (1986). See especially p. 268.
10. "On the Rates of Radiation Events in CCD's (Excerpt from an ESO report)," available at `http://www.pv-inc.com/tutorial/tutorial.htm`.
11. R. Florentin-Nielsen, M. I. Andersen, & S. P. Nielsen, "Cosmic ray events and natural radioactivity in CCD cryostats," in *New developments in Array Technology and Applications*, eds. A. G. Philip et al., IAU Symp 167 (1995).
12. D. Walton, R. A. Stern, R. C. Catura, & J. L. Culhane, SPIE **501**, 306–316 (1984).
13. O.C. Allkofer, K. Carstensen, and W.D. Dau, Phys. Lett. **B36**,425 (1971).
14. B.C. Rastin, J. Phys. **G10**, 1609 (1984).
15. *American Institute of Phyics Handbook*, 3rd ed., edited by E. D. Gray (McGraw-Hill, New York, 1972).
16. D.E. Groom, N.V. Mokhov, and S.I. Striganov, "Muon stopping-power and range tables," Atomic Data and Nuclear Data Tables **78**, 183–356 (2001).
17. F. Scholze, H. Rabus, & G. Ulm, J. App. Phys. **84**, 2926–2939 (1998); F. Scholze, H. Henneken, P. Kuschnerus, H. Rabus, & G. Ulm, Nucl. Instrum. Methods **A439**, 208–215 (2000); F. Scholze, private communication, 27 Sept 2000, discusses the temperature dependance of the mean energy per e-h pair, and concludes that the value 3.66 eV/e-h should scale to 3.73 eV/e-h at 200 K and 3.79 eV/e-h at 100 K. We interpolate to 3.77 eV/e-h at $-100°$ C.
18. H. Bichtel, Rev. Mod. Phys. **60**, 663–699 (1988).